

Supplementary Materials for
Integrated single-cell RNA-seq analysis reveals mitochondrial calcium signaling as a modulator of endothelial-to-mesenchymal transition

Mathilde Lebas *et al.*

Corresponding author: Anna Rita Cantelmo, anna-rita.cantelmo@univ-lille.fr

Sci. Adv. **10**, eadp6182 (2024)
DOI: 10.1126/sciadv.adp6182

The PDF file includes:

Figs. S1 to S8
Legends for tables S1 to S7

Other Supplementary Material for this manuscript includes the following:

Tables S1 to S7

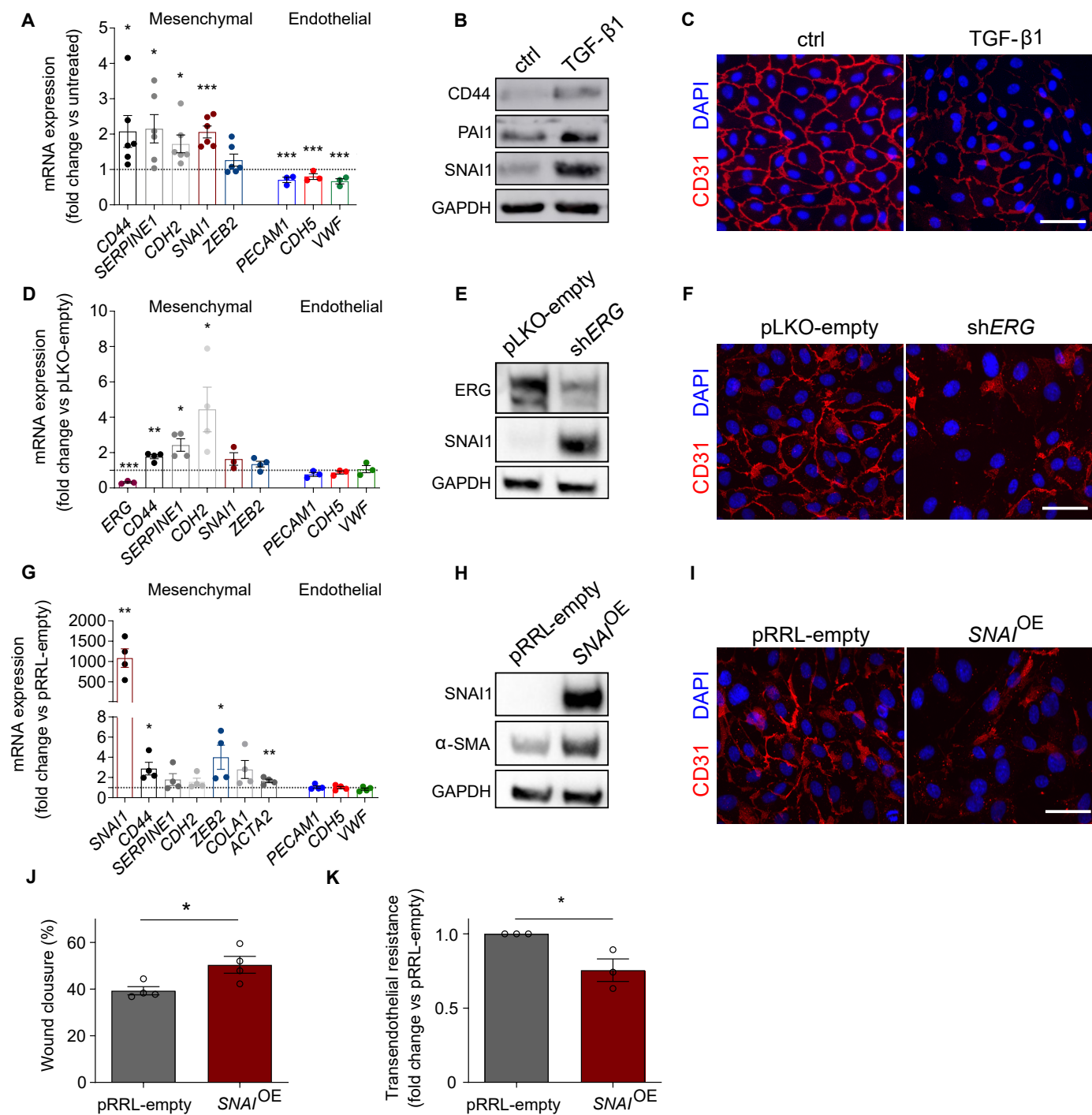
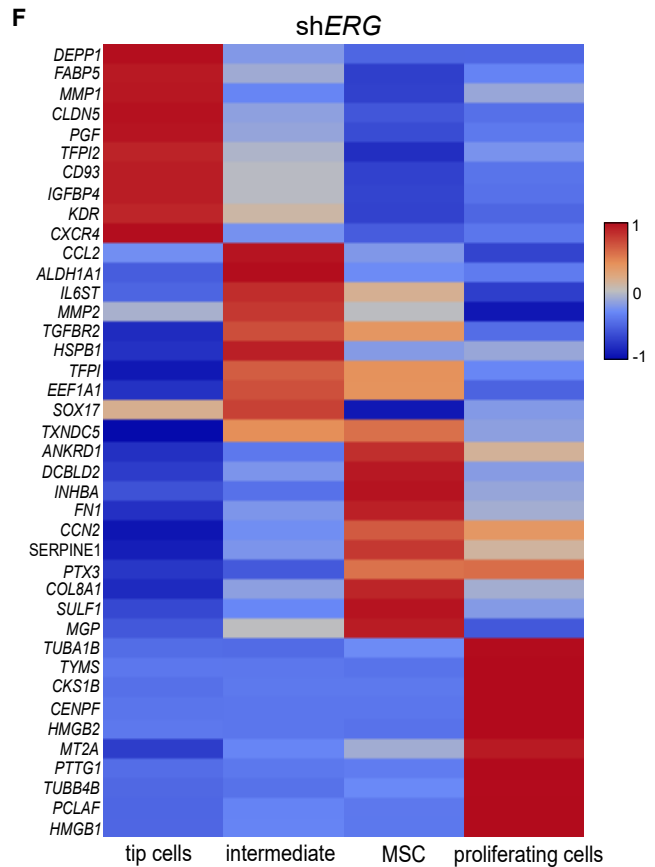
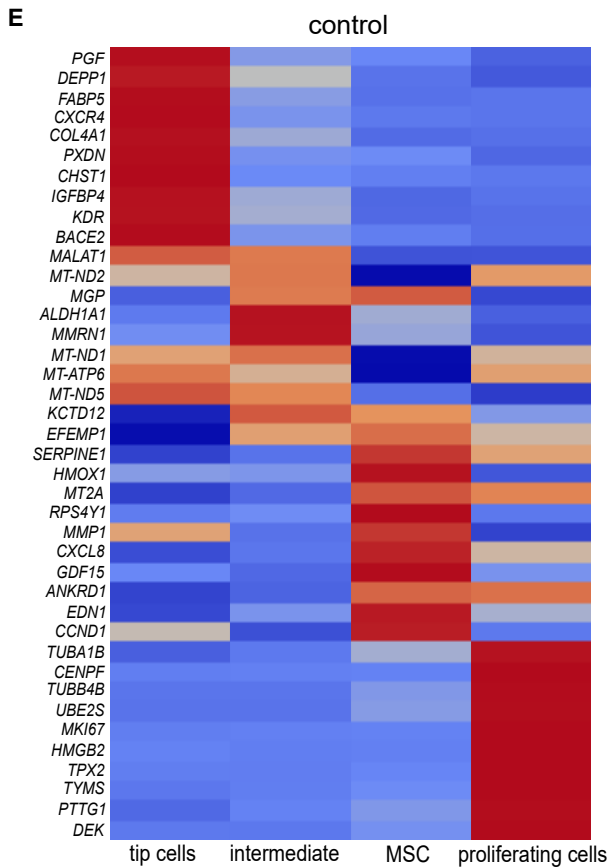
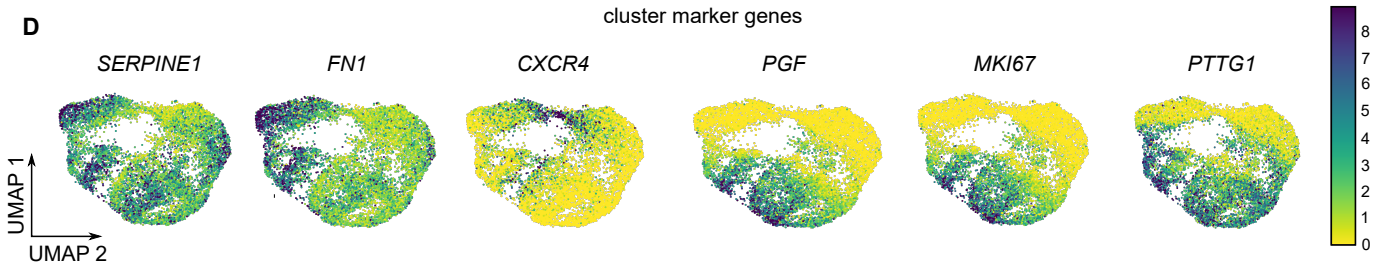
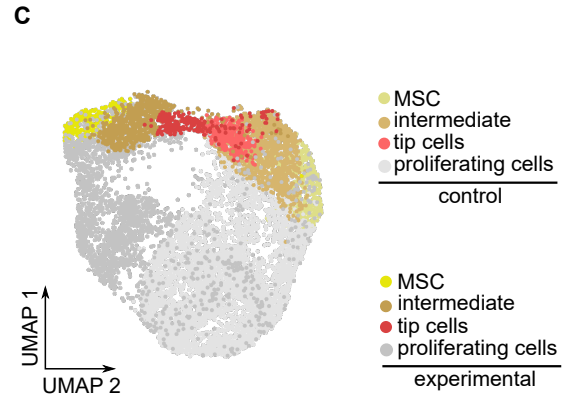
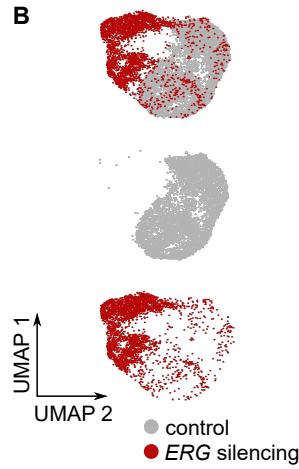
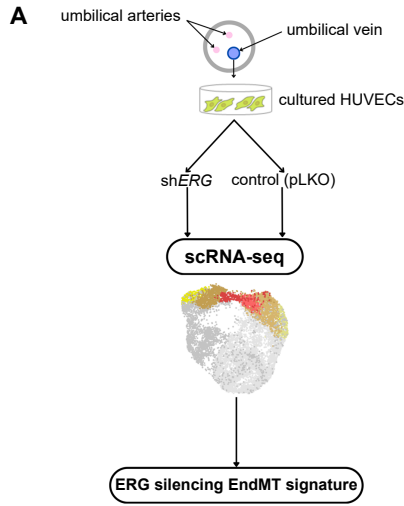


Fig. S1. In vitro EndMT induction. (A) RT-PCR analysis of mRNA expression levels of mesenchymal and endothelial genes in TGF- β -treated ECs compared to control ECs. Expression values were normalized to 18S mRNA levels and they are relative to untreated control (N= 3-6). Dotted line: expression levels in untreated ECs. *P value < 0.05, ***P < 0.001. (B) Representative immunoblots for CD44, PAI, SNAI1 and GAPDH in cytosolic fractions in control and TGF- β 1-treated ECs. (C) CD31 staining of control and TGF- β 1-treated ECs. Nuclei are counterstained with DAPI (blue). Scale bar, 50 μ m. (D) RT-PCR analysis of mRNA expression levels of mesenchymal and endothelial genes in shERG compared to non-silenced control ECs (pLKO-empty). Expression values were normalized to 18S mRNA levels and they are relative to non-silenced control (N= 3-4). Dotted line: expression levels in pLKO-empty. *P value < 0.05, **P < 0.01, ***P < 0.001. (E) Representative immunoblots for ERG, SNAI1 and GAPDH in cytosolic fractions in shERG and non-silenced control (pLKO-empty). (F) CD31 staining of shERG and non-silenced control (pLKO-empty). Nuclei are counterstained with DAPI (blue). Scale bar, 50 μ m. (G) RT-PCR analysis of mRNA expression levels of mesenchymal and endothelial genes in SNAI^{OE} compared to control ECs (pRRL-empty). Expression values were normalized to 18S mRNA levels and they are relative to non-overexpressing control (N= 4). Dotted line: expression levels in pRRL-empty. *P value < 0.05, **P < 0.01. (H) Representative immunoblots for SNAI1, α -SMA and GAPDH in cytosolic fractions in SNAI^{OE} and control (pRRL-empty). (I) CD31 staining of SNAI^{OE} and control (pRRL-empty). Nuclei are counterstained with DAPI (blue). Scale bar, 50 μ m. (J) Quantification of scratch wound assay using mitomycin C-treated control (pRRL-empty) and SNAI^{OE} (N= 4). *P < 0.05. (K) Transendothelial electrical resistance of control (pRRL-empty) and SNAI^{OE} EC monolayers (N= 3). *P value < 0.05.



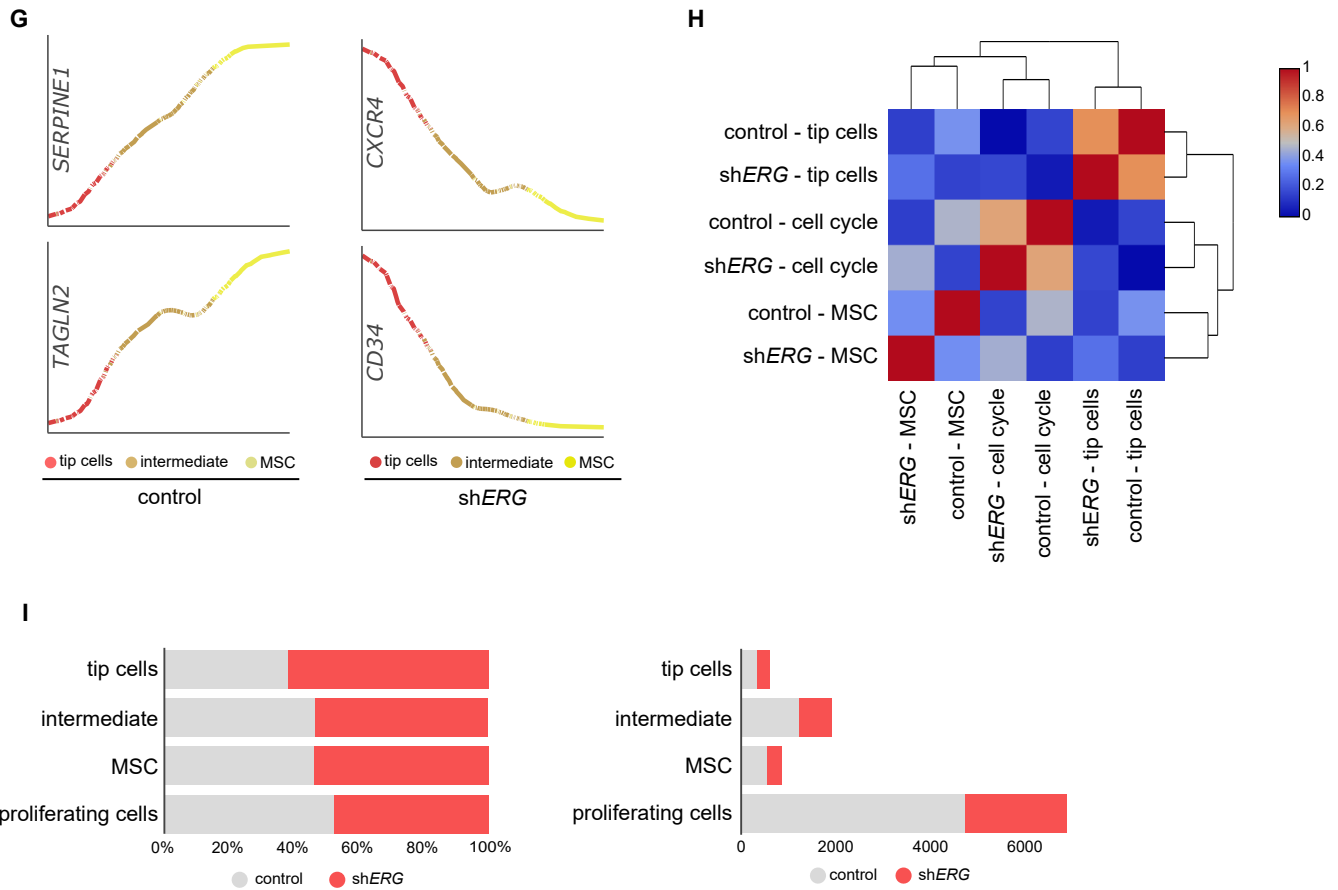
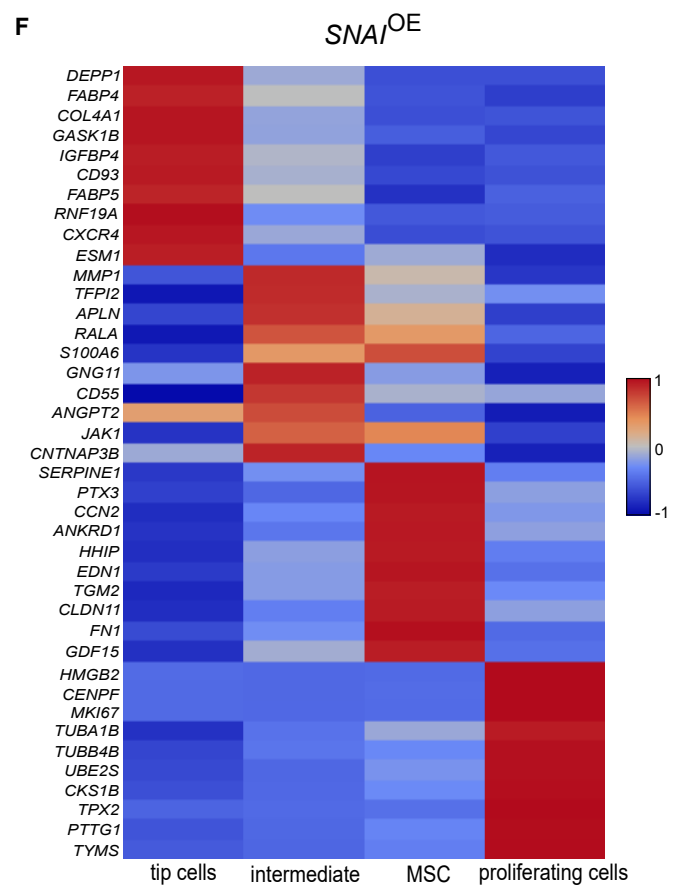
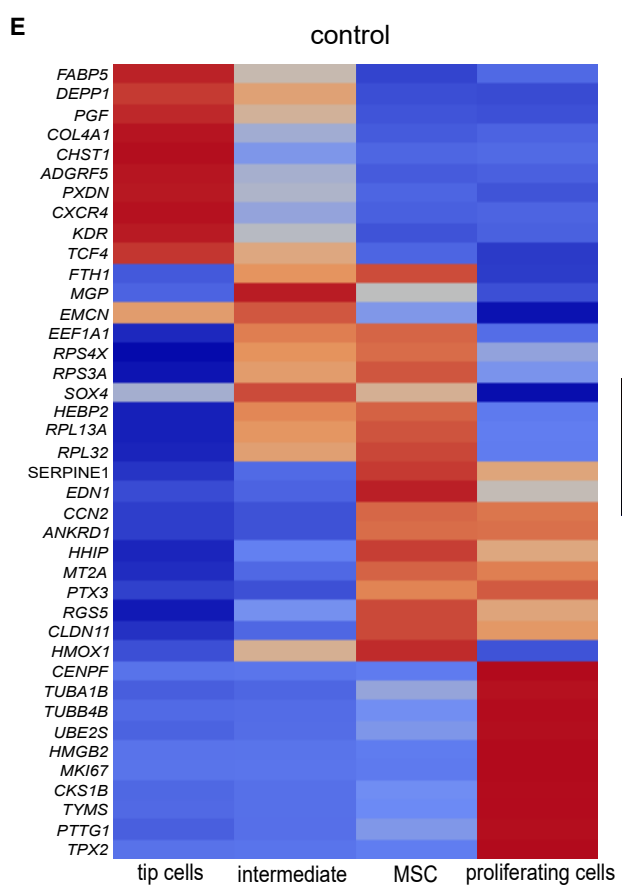
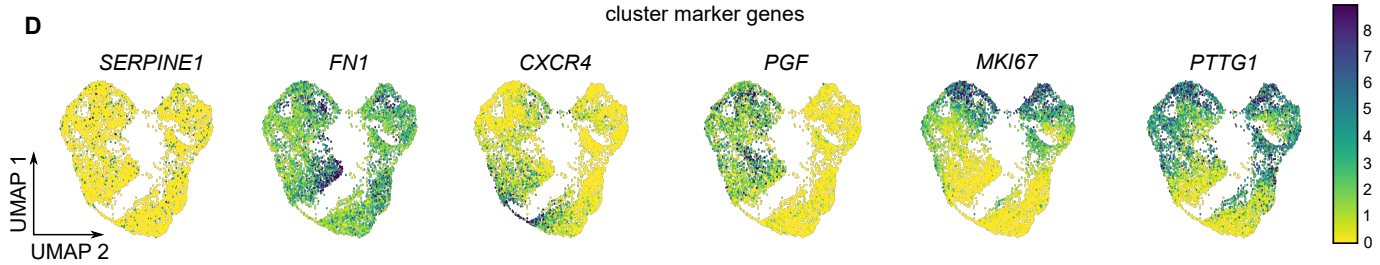
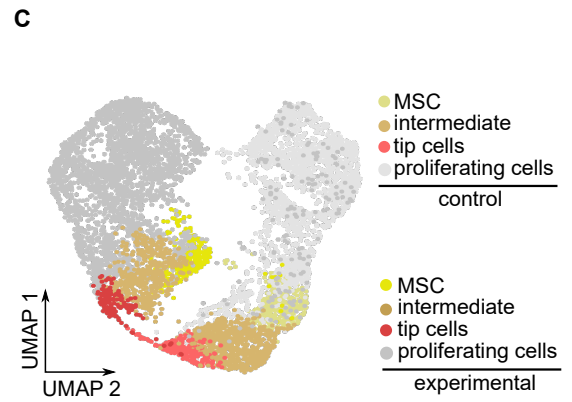
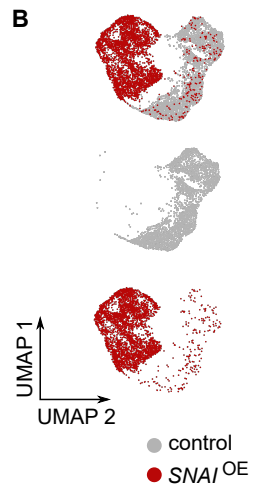
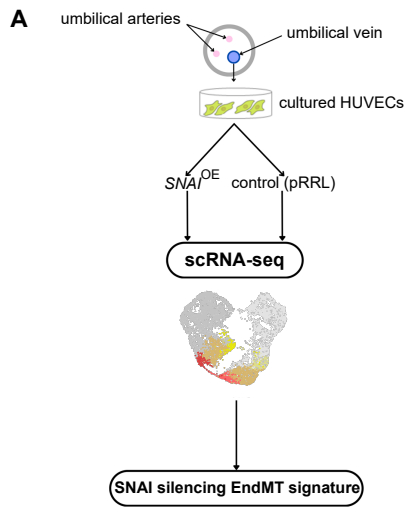


Fig. S2. scRNA-seq analysis for the shERG model. (A) Graphical representation of the experimental design for the *ERG* silencing model. (B) UMAP showing separation of cells based on condition. (C) UMAP analysis of 10,225 cultured HUVECs from the *ERG* silencing experiment. (D) UMAP plots color-coded for the indicated marker genes. (E) Heatmap analysis of top 10 uniquely upregulated cluster marker genes in control (pLKO-empty) and shERG (F). (G) Pseudotime analysis of canonical tip and MSC genes. (H) Dendrogram visualization of hierarchical clustering analysis on gene signature correlations of top 10 annotated clusters marker genes. Note: marker genes for the intermediate cluster were not calculated since it represents a transitional phase between tip cells and MSC. (I) Cell type quantification per annotated cluster and condition expressed in relative (top) and absolute (bottom) numbers.



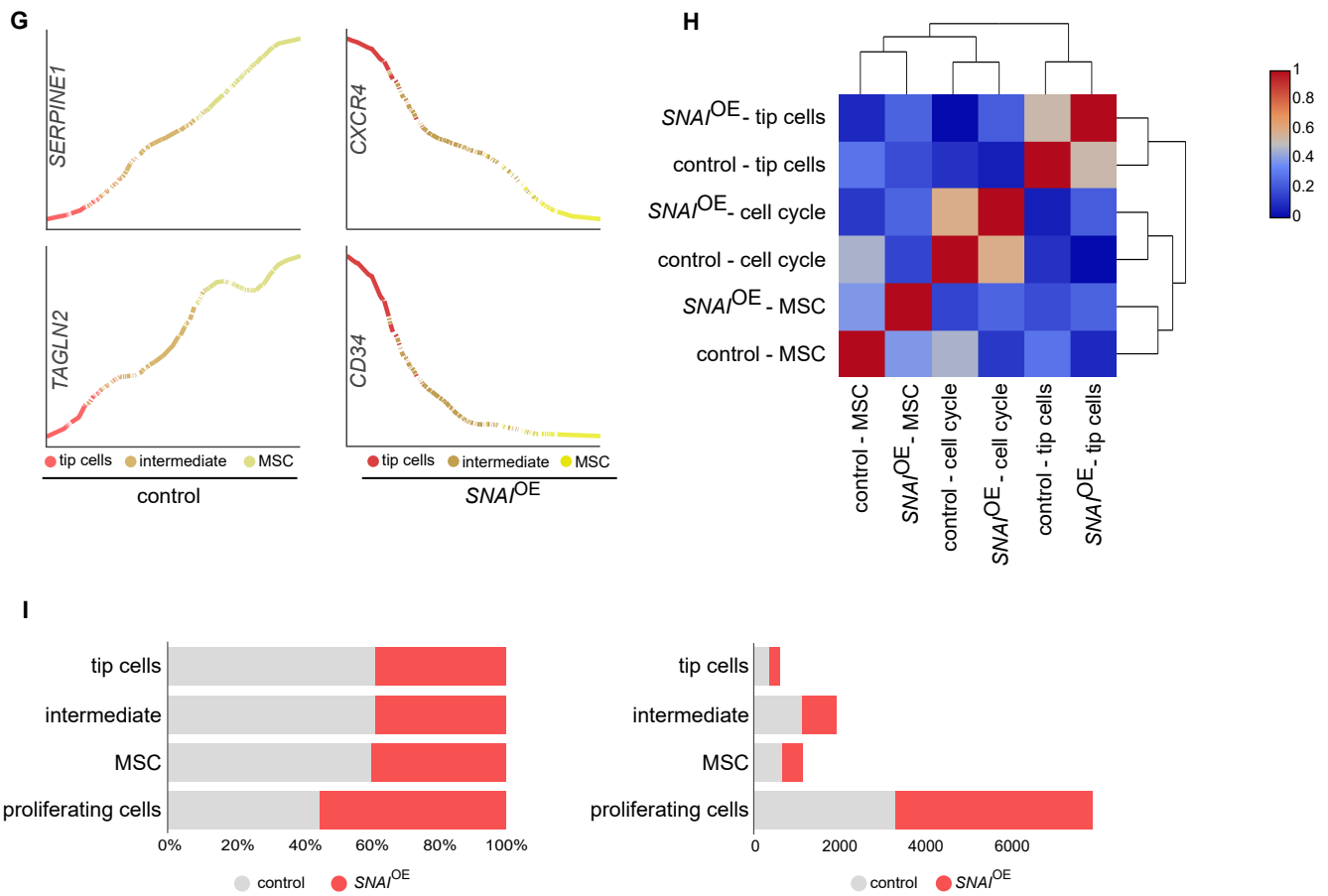
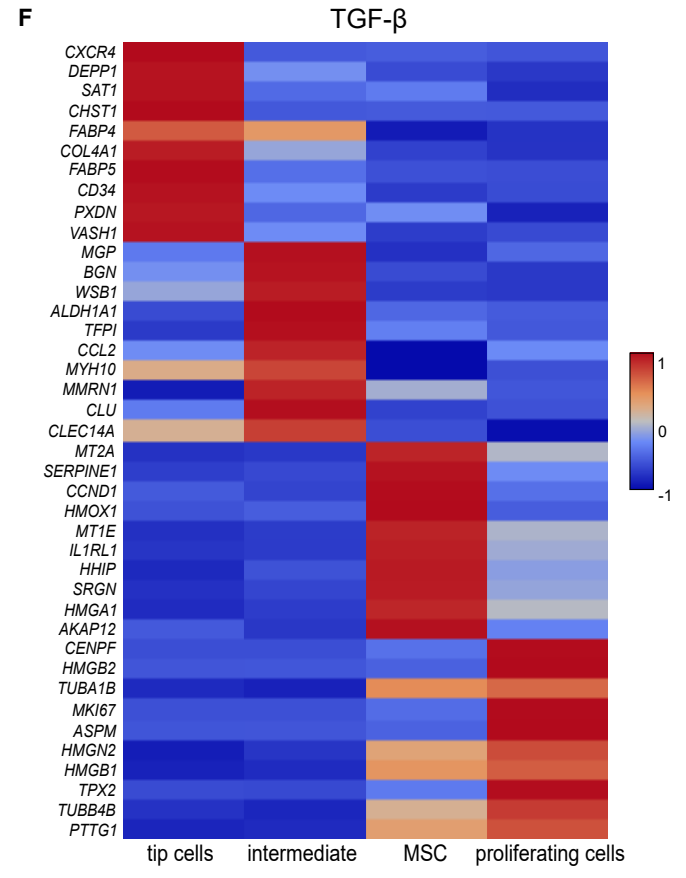
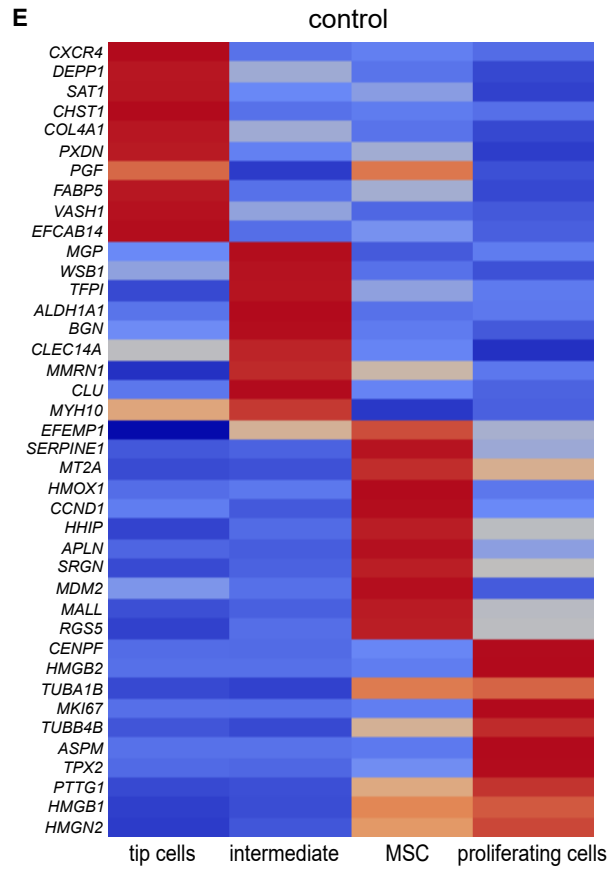
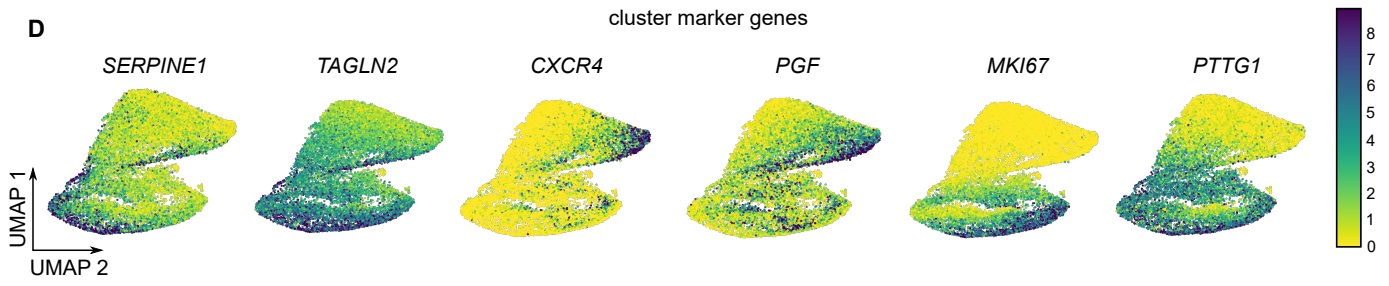
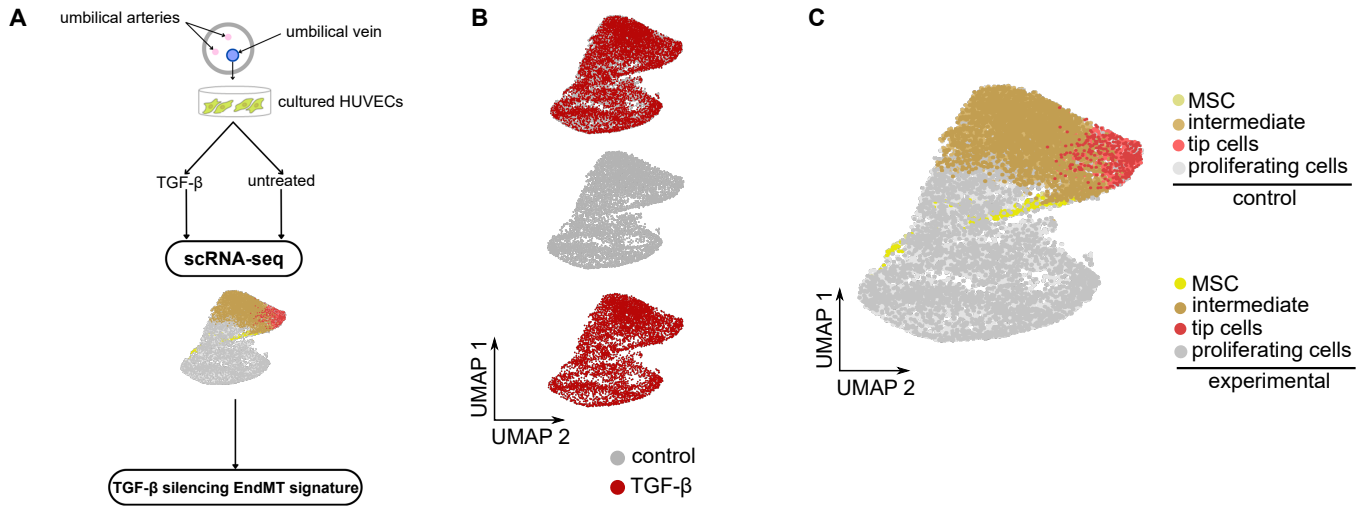


Fig. S3. scRNA-seq analysis for the SNA1^{OE} model. (A) Graphical representation of the experimental design for the SNA1 overexpression model. (B) UMAP showing separation of cells based on condition. (C) UMAP analysis of 7,298 cultured HUVECs from the SNA1 overexpression experiment. (D) UMAP plots color-coded for the indicated marker genes. (E) Heatmap analysis of top 10 uniquely upregulated cluster marker genes in control (pRRL-empty) and SNA1^{OE} (F). (G) Pseudotime analysis of canonical tip and MSC genes. (H) Dendrogram visualization of hierarchical clustering analysis on gene signature correlations of top 10 annotated clusters marker genes. Note: marker genes for the intermediate cluster were not calculated since it represents a transitional phase between tip cells and MSC. (I) Cell type quantification per annotated cluster and condition expressed in relative (top) and absolute (bottom) numbers.



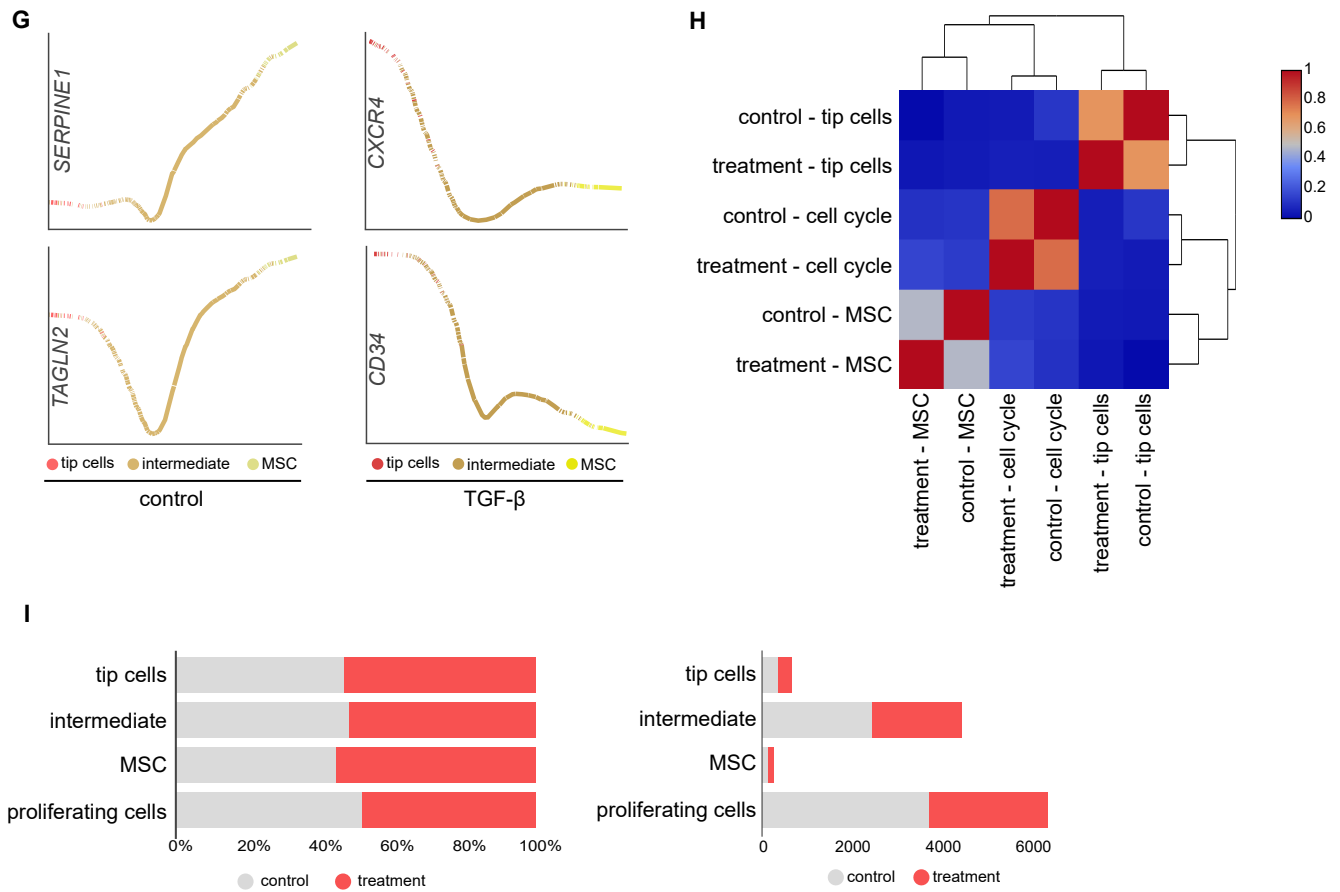
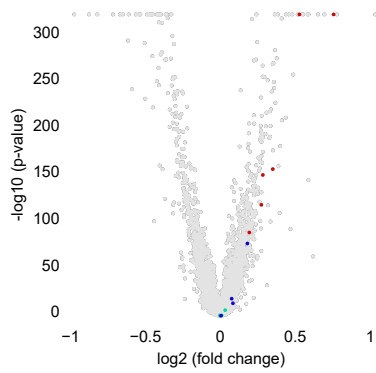


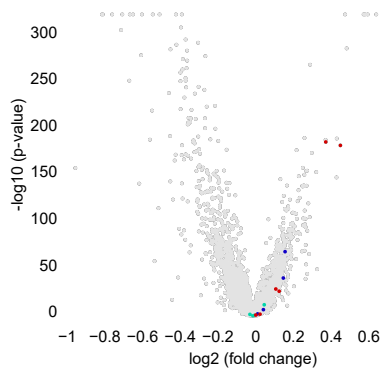
Fig. S4. scRNA-seq analysis for the TGF- β model. (A) Graphical representation of the experimental design for the TGF- β model. (B) UMAP showing separation of cells based on condition. (C) UMAP analysis of 14,602 cultured HUVECs from the TGF- β experiment. (D) UMAP plots color-coded for the indicated marker genes. (E) Heatmap analysis of top 10 uniquely upregulated cluster marker genes in control (untreated) and TGF- β (F). (G) Pseudotime analysis of canonical tip and MSC genes. (H) Dendrogram visualization of hierarchical clustering analysis on gene signature correlations of top 10 annotated clusters marker genes. Note: marker genes for the intermediate cluster were not calculated since it represents a transitional phase between tip cells and MSC. (I) Cell type quantification per annotated cluster and condition expressed in relative (top) and absolute (bottom) numbers.

A DGEA - control vs experimental proliferating cells (*shERG*)

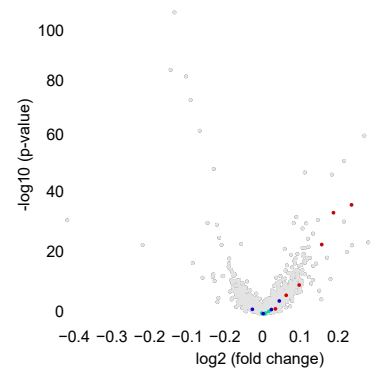


● endoplasmic reticulum lumen ● sarcoplasmic reticulum lumen ● MCU complex

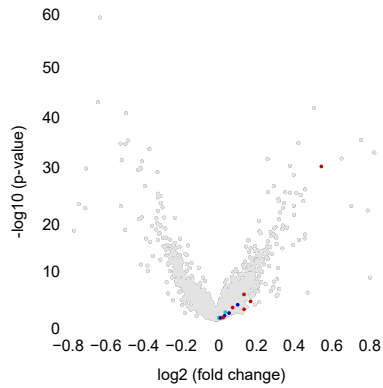
B DGEA - control vs experimental proliferating cells (*SNAI1^{OE}*)



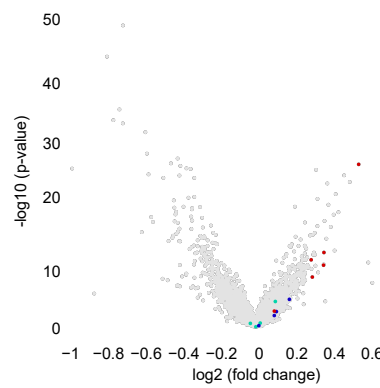
C DGEA - untreated vs treatment proliferating cells (*TGF-β*)



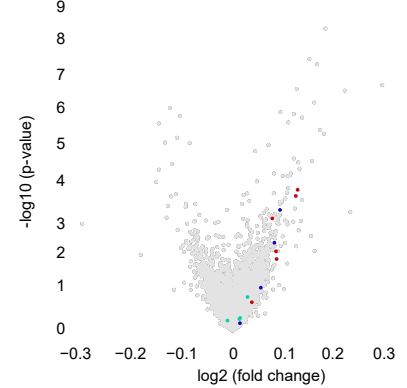
D DGEA - control vs experimental tip cells (*shERG*)



E DGEA - control vs experimental tip cells (*SNAI1^{OE}*)

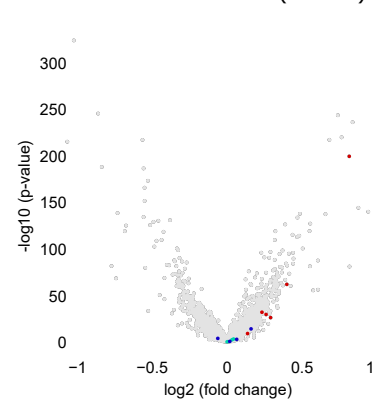


F DGEA - untreated vs treatment tip cells (*TGF-β*)

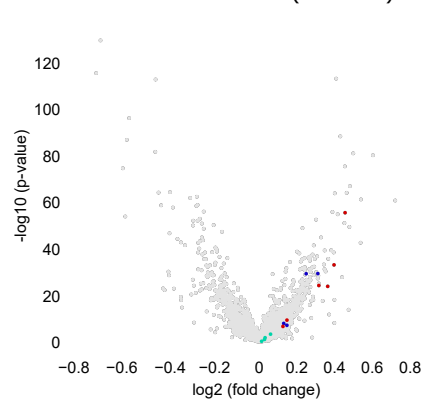


● endoplasmic reticulum lumen ● sarcoplasmic reticulum lumen ● MCU complex

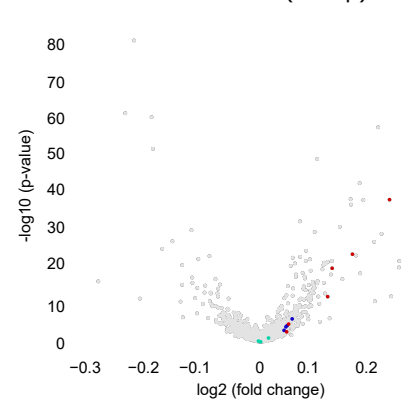
G DGEA - control vs experimental intermediate cells (*shERG*)



H DGEA - control vs experimental intermediate cells (*SNAI1^{OE}*)



I DGEA - untreated vs treatment intermediate cells (*TGF-β*)



● endoplasmic reticulum lumen ● sarcoplasmic reticulum lumen ● MCU complex

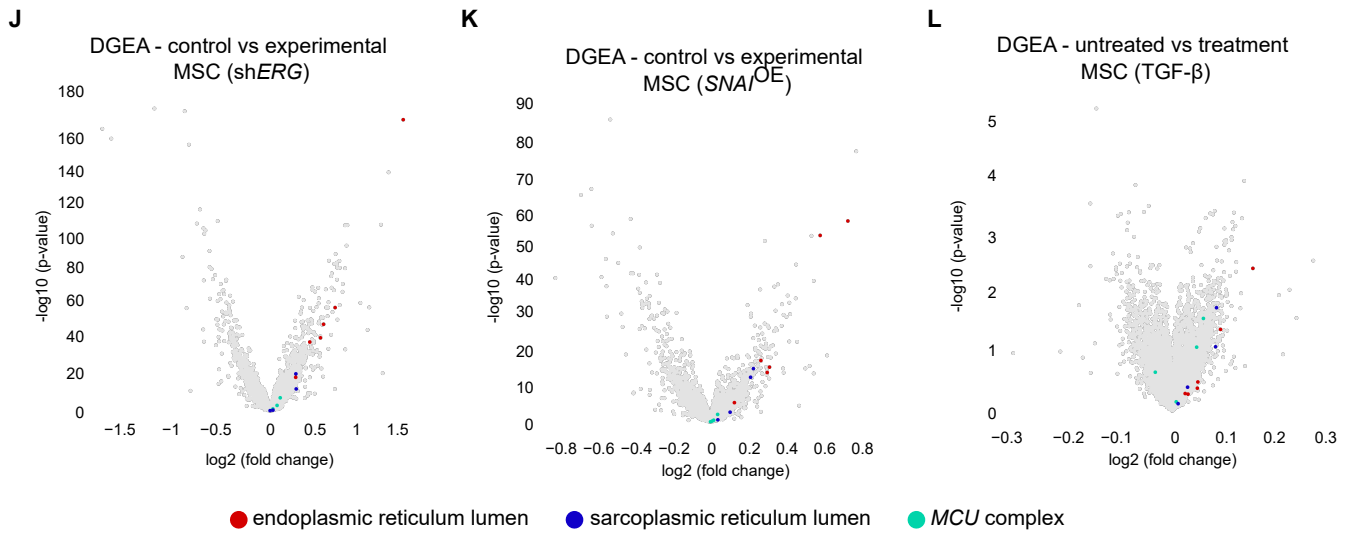
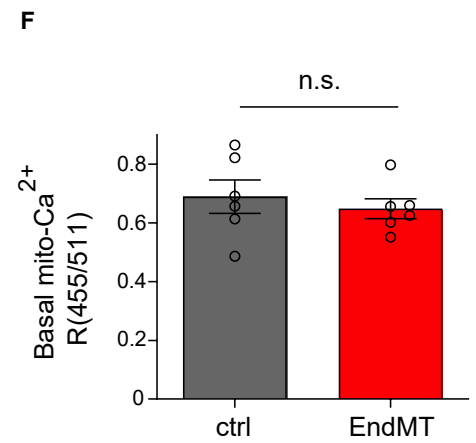
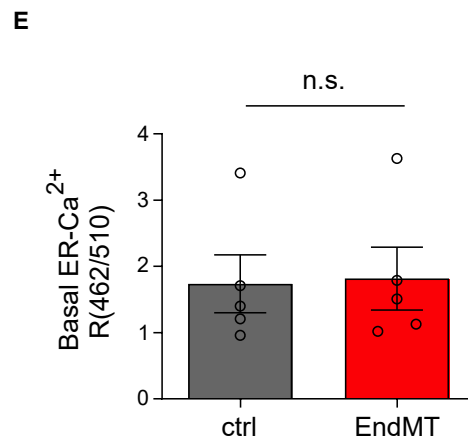
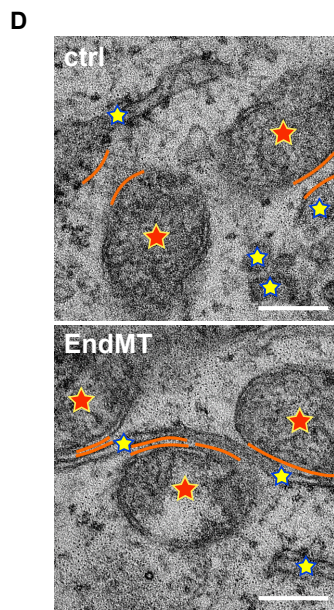
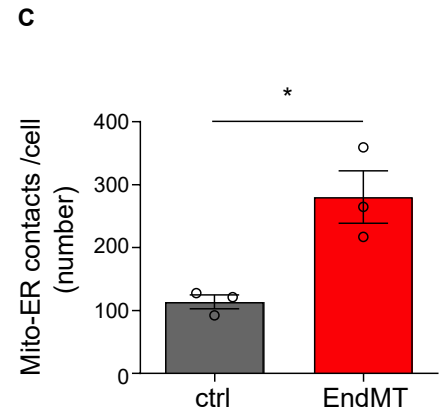
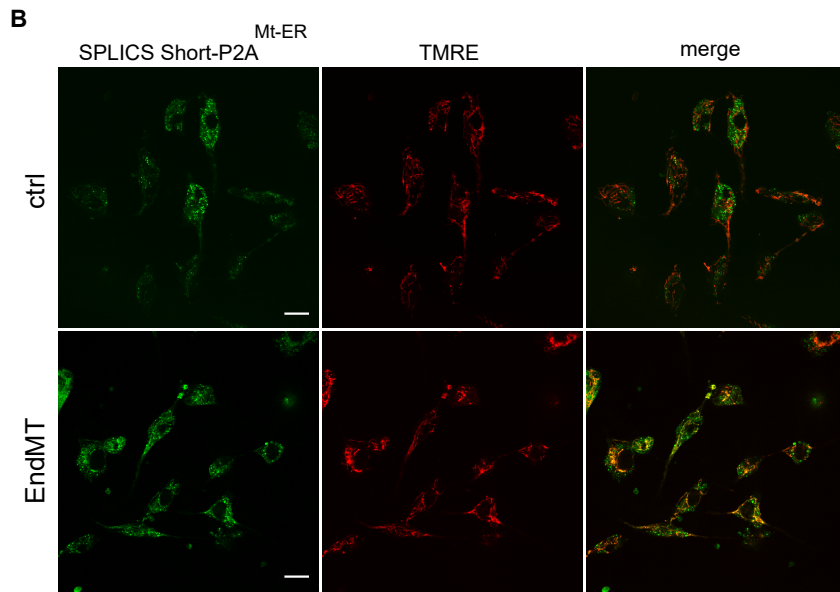
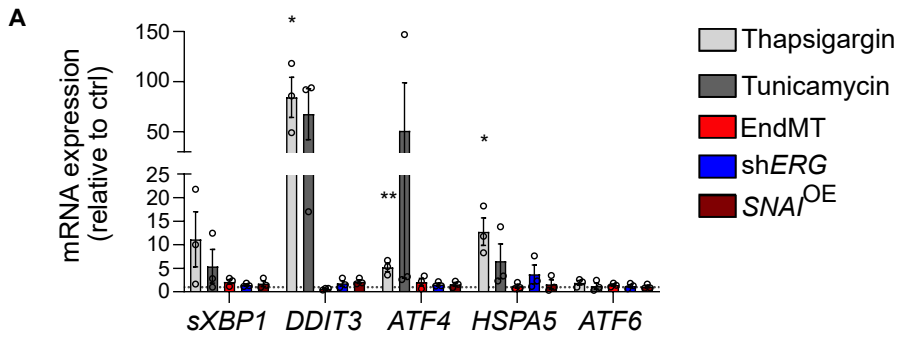


Fig. S5. Comparison between control and experimental condition (EndMT induction) on different levels. (A) Volcano plot of a differential analysis of control vs experimental condition for proliferating cells in shERG (A), *SNAI1*^{OE} (B) and TGF- β treatment (C). Volcano plot of a differential analysis of control vs experimental condition for tip cells in shERG (D), *SNAI1*^{OE} (E) and TGF- β treatment (F). Volcano plot of a differential analysis of control vs experimental condition for intermediate state in shERG (G), *SNAI1*^{OE} (H) and TGF- β treatment (I). Volcano plot of a differential analysis of control vs experimental condition for MSC in shERG (J), *SNAI1*^{OE} (K) and TGF- β treatment (L). The endoplasmic reticulum lumen genes are in red outline; the sarcoplasmic reticulum lumen genes are highlighted in blue; *MCU* complex genes are highlighted in green.



★ Mitochondria
 ★ Cisternal space of rough endoplasmic reticulum
 — Mitochondria-associated ER Membrane

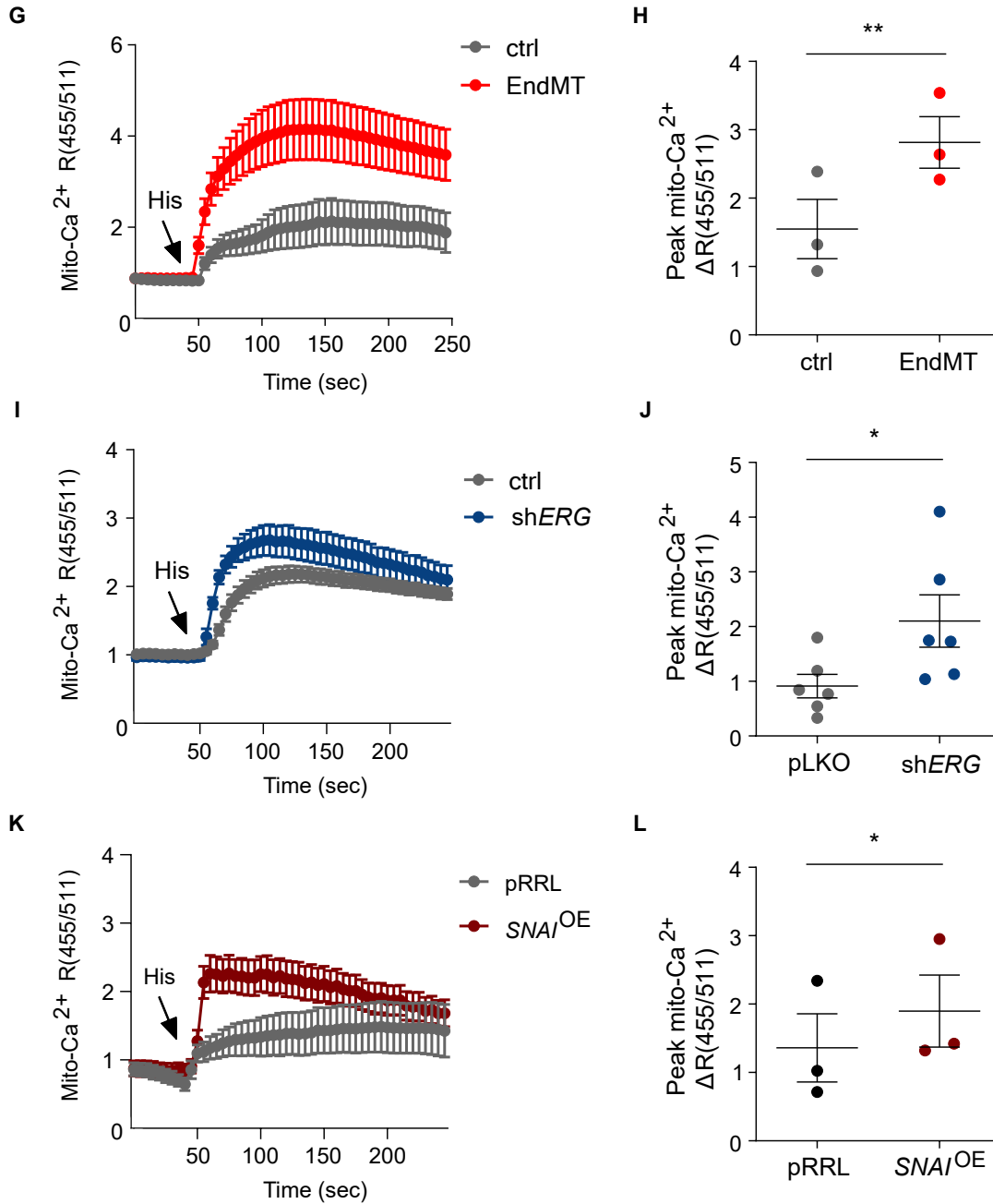
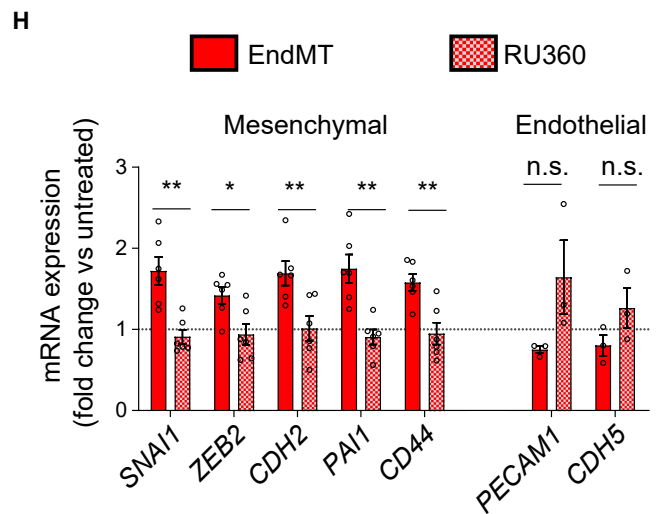
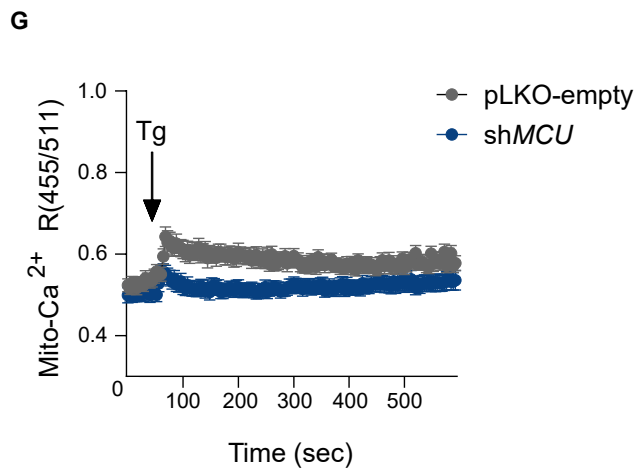
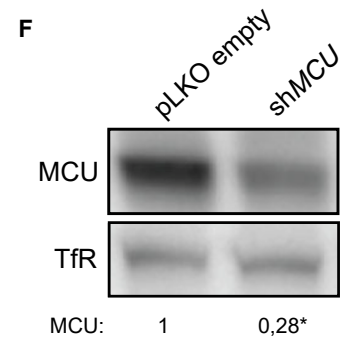
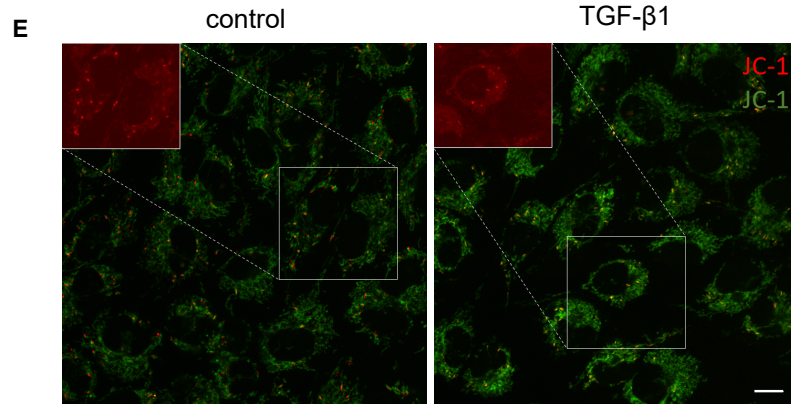
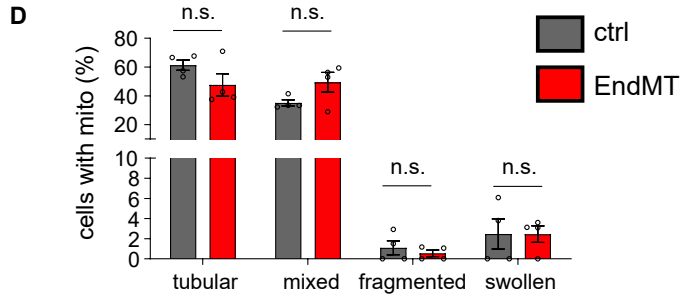
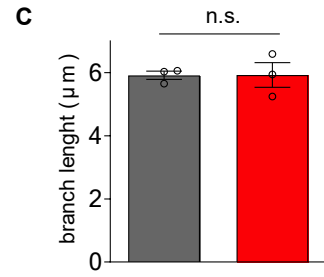
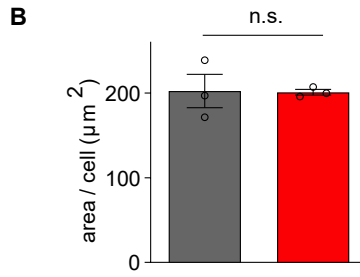
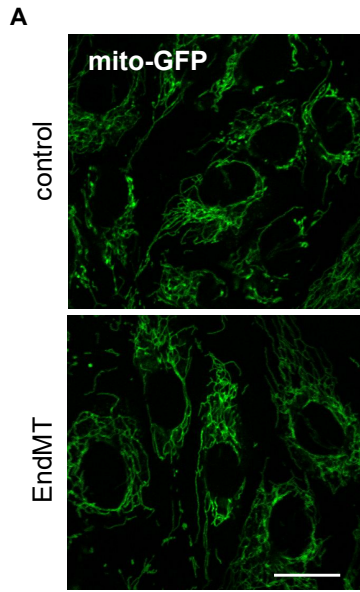


Fig. S6. EndMT is associated with increased mitochondrial Ca^{2+} uptake. (A) RT-PCR analysis of mRNA expression levels of ER stress genes in the three EndMT models. Thapsigargin (10 μM) and tunicamycin (5 $\mu\text{g}/\text{ml}$) were used as ER stressors over 4 hours (positive controls). Expression values were normalized to 18S mRNA levels and they are relative to control (for EndMT models) or untreated (for positive controls) (N= 3). Dotted line: expression levels in control ECs. *P value < 0.05, ***P < 0.01. (B) Representative images of mitochondrial-ER contact sites in control and EndMT-derived cells (TGF- β 1 stimulation) expressing the SPLICSS probe (SPLICSS Short-P2A^{Mt-ER} in green). Mitochondria were visualized by TMRE (red). (C) Quantification of B. The SPLICSS dots were quantified from the 3D rendering of a complete z-stack (N= 3). *P value < 0.05. Scale bar 20 μm . (D) Electron micrographs of control and EndMT-derived cells (TGF- β 1 stimulation) showing mitochondrial-associated ER membranes (orange lines). Red stars represent mitochondria, yellow stars cisternal space of rough ER. Scale bar, 200 nm. Quantification of basal ER- Ca^{2+} (E) and mito- Ca^{2+} (F) levels in control and EndMT-derived cells (TGF- β 1 stimulation) transduced with the ER-targeted or mitochondria-targeted ratiometric Ca^{2+} sensors GEM-Cepia1er and GEM-Geco1mito, respectively and maintained in 0 mM extracellular Ca^{2+} solution (N= 5 for ER- Ca^{2+} ; n=6 for mito- Ca^{2+}). n.s.: no significance. (G-L) Imaging traces and quantification of mito- Ca^{2+} levels in response to histamine (His, 50 μM) in control and EndMT-derived cells in 2 mM extracellular Ca^{2+} solution in the three models. Traces (G-I-K) represent the mean Geco ratio (455/511 nm) \pm SEM of different cells from one representative experiment. The scatter dot plots (H-J-L) show the mean peak amplitude \pm SEM of His-mediated mitochondrial Ca^{2+} uptake relative to three (TGF- β and SNAI^{OE}) or six (shERG) independent experiments. *P value < 0.05, **P value < 0.01.



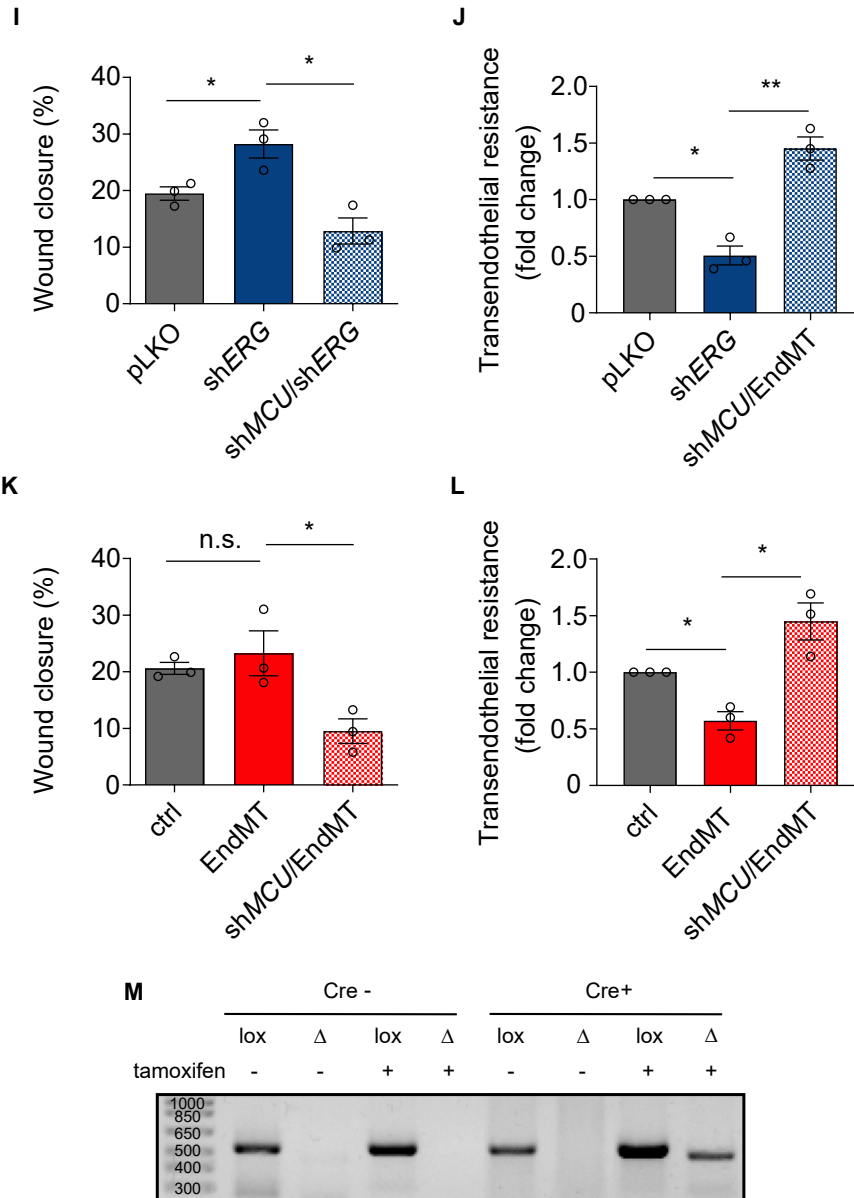


Fig. S7. MCU overexpression regulates EndMT. (A-D) Representative images and relative quantification of mitochondrial morphology in control and EndMT-derived cells (TGF- β 1 stimulation) transduced with a mito-GFP reporter (N= 3-4). n.s.: no significance. Scale bar, 20 μ m. (E) Representative images of control (ctrl) and TGF- β 1-treated ECs stained for the JC-1 dye. Red fluorescence emission of the dye is indicative of potential-dependent accumulation of JC-1 in the mitochondria (associated with a fluorescence emission shift from green (520-550 nm) to red (579-633 nm)). Insets in the single channel JC-1 red panels show larger magnifications of the boxed areas to visualize presence of red aggregates. Scale bar, 10 μ m. (F) Representative expression levels and relative quantification of immunoblot for MCU in control ECs (pLKO-empty) and ECs transduced with a shRNA targeting MCU (shMCU1). Transferrin receptor (TfR) was used as loading control (N= 3). *P value < 0.05. (G) Mito-Ca²⁺ imaging traces in response to thapsigargin (Tg, 2 μ M) in control cells (black trace) and in cells silenced for MCU (shMCU1/shMCU2, blue trace) maintained in 0 mM extracellular Ca²⁺ solution. Traces on the left represent the mean Geco ratio (455/511 nm) \pm SEM of different cells from one representative experiment of N= 6. (H) RT-PCR analysis of mRNA expression levels of mesenchymal and endothelial genes in untreated vs ECs treated with RU360 (1 μ M) prior EndMT induction by TGF- β 1 stimulation. Expression values were normalized to 18S mRNA levels (N= 3-6). Dotted line: expression levels in untreated EndMT. *P value < 0.05, **P < 0.01, n.s.: no significance. (I) Quantification of scratch wound assay using mitomycin C-treated control (pLKO-empty) and shERG (N= 3). *P < 0.05. (J) Transendothelial electrical resistance of control (pLKO-empty) and shERG monolayers (N= 3). *P value < 0.05, **P < 0.01. (K) Quantification of scratch wound assay using mitomycin C-treated control (ctrl) and EndMT-derived cells (TGF- β 1 stimulation) (N= 3). *P < 0.05, n.s.: no significance. (L) Transendothelial electrical resistance of control (ctrl) and EndMT-derived cells (TGF- β 1 stimulation) (N= 3). *P < 0.05. (M) Correct recombination of the lox allele in WT (Cre-) and *Snai1*^{ECKO} (Cre+) mice upon tamoxifen (Tam) treatment, as assessed by genomic DNA PCR. PCR to amplify the loxP-flanked *Snai1* allele (lox) or the Cre-recombined allele (Δ) were run and loaded in separate reactions. The gel picture shown is representative of all WT and *Snai1*^{ECKO} mice used in this study.

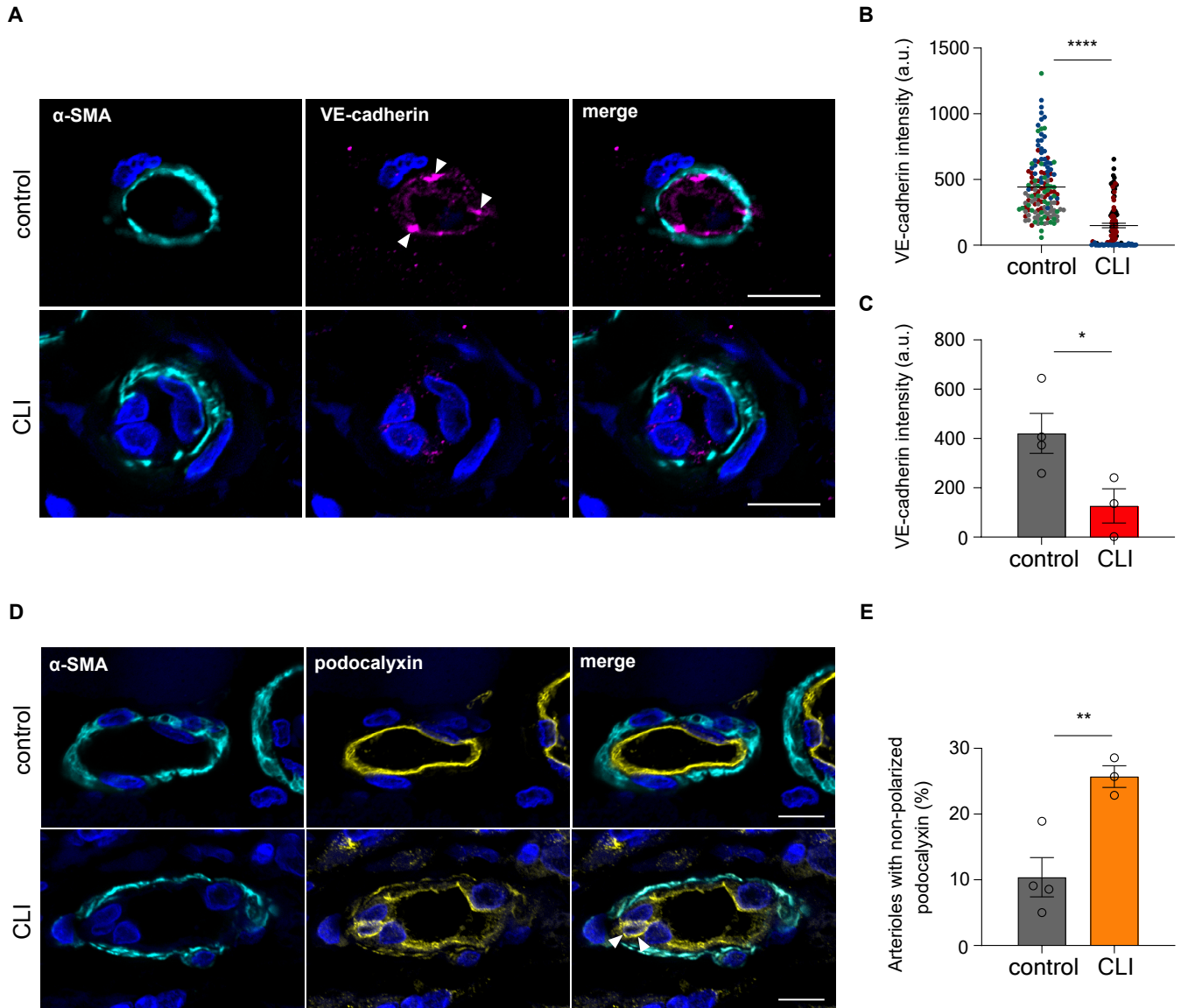


Fig. S8. ECs in CLI muscle display EndMT features. (A) Confocal micrographs in human skeletal muscle from control individuals and individuals with critical limb ischemia (CLI) stained for mural cells (α -SMA, cyan), VE-cadherin (magenta), and nuclei (DAPI, blue). Scale bars, 10 μ m. Control arterioles show junctional enrichment of VE-cadherin (arrows), whereas CLI arterioles show weak and diffuse VE-cadherin signals. (B) Quantification of VE-cadherin in individual arterioles (median intensity and interquartile range, 140 and 105 arterioles, respectively) and per subject (C) (Mean \pm SEM). * $P < 0.05$, **** $P < 0.0001$. (D) Confocal micrographs of small arterioles stained for mural cells (α -SMA, green), podocalyxin (yellow), and nuclei (DAPI, blue). Scale bars, 10 μ m. CLI arterioles show ECs with variably located podocalyxin including at lateral and basal locations (arrows). (E) Quantification of A depicting the percent of arterioles per subject with non-polarized podocalyxin (N= 4 for control and N= 3 for CLI patients). Data are mean \pm SEM. ** $P < 0.01$.

Supplementary tables

Table S1. scRNA-seq quality control metrics.

Table S2 (related to Fig. 1B and Figures S2A-D, S3A-D and Fig. S4A-D). Uniquely upregulated cluster marker genes characterizing the four different EC subpopulations.

Table S3 (related to Fig. 1D-F). Congruent genes in the top 100 marker genes of proliferating, tip and MSC.

Table S4 (related to Fig. S5). Differential gene expression analyses comparing cell clusters in control vs experimental conditions. Gene lists are ranked according to log₂ fold change and used as input for the cell cluster-independent meta-analysis.

Table S5 (related to Fig. 3A). Congruently upregulated genes in EndMT induction independent of the cell cluster.

Table S6 (related to Fig. 3B). Cell cluster-independent EndMT meta-analysis.

Table S7 (related to Fig. 4A-C). Results of GOrilla cellular component GO analysis.